Shock synthesis of Al-Fe-Cr-Cu-Ni icosahedral quasicrystal

Cite as: AIP Conference Proceedings **2272**, 100013 (2020); https://doi.org/10.1063/12.0001005
Published Online: 04 November 2020

Jinping Hu, Paul D. Asimow, and Chi Ma

Shock Synthesis of Al-Fe-Cr-Cu-Ni Icosahedral Quasicrystal

Jinping Hu[1, a)], Paul D. Asimow[1, b)] and Chi Ma[1, c)]

[1]*Division of Geological and Planetary Sciences, California Institute of Technology, 1200 E California Blvd, Pasadena CA 91125, USA*

[a)]Corresponding author: jinping@caltech.edu
[b)]asimow@gps.caltech.edu
[c)]chi@gps.caltech.edu

Abstract. Al-alloy quasicrystals (QC) are of great interest because of their unique physical properties and natural occurrence in a meteorite. Considerable effort has been invested to explore the compositional fields of stable QC and quenchable metastable QC. In this light, shock recovery experiments, originally aimed at proving the planetary impact origin of natural quasicrystalline phases, also offer a novel strategy for synthesizing novel QC compositions and exploring expanded regions of the QC stability field. In this study, we shocked an Al-Cu-W graded density target (originally manufactured for use as a ramp-generating impactor but here used as target) to sample interactions between 304 stainless steel and the full range of Al/Cu starting ratios. This experiment synthesized an icosahedral quasicrystal of new composition $Al_{68}Fe_{20}Cr_6Cu_4Ni_2$. No previous reports of Al-Fe-Cr QCs have reached such high Fe/Cr ratio or low Al content. The Cr+Ni content is at the upper bound of this low-Cu quinary icosahedral QC according the Hume-Rothery rules for stability. Our synthesis suggests that the presence of Cu promotes the incorporation of Cr+Ni in the Al-rich icosahedral QC phase, enabling the high Fe/Cr ratio observed.

INTRODUCTION

Quasicrystals (QC) are a unique type of solid with quasi-periodicity and forbidden crystallographic symmetries. The first known quasicrystal, e.g., has an Al-Mn binary composition and icosahedral symmetry featuring 5-fold, 3-fold and 2-fold rotation axes [1]. Since the discovery of the first QC, a number of QCs in Al-TM (transition metal) binary, ternary and quaternary systems has been synthesized at ambient pressure [2]. Recent exploration of the stability of quasicrystal during shock compression was motivated by the discovery of both $Al_{63}Cu_{25}Fe_{12}$ icosahedral quasicrystal (i-QC) and $Al_{71}Ni_{24}Fe_5$ decagonal QC in the Khatyrka meteorite [3,4]. The natural discovery presents a puzzle because the conditions and procedures used in laboratory synthesis of QC [2] from metallic liquid, gas or glass hardly resemble any natural rock-forming processes. The successful synthesis of Al-Cu-Fe i-QC in shock recovery experiments therefore unambiguously supported a planetary impact origin for the natural meteoritic QCs [5]. Moreover, the shock experiments produced quinary Al-Cu-Fe-Cr-Ni i-qc with compositions that have not been observed at ambient pressure [6]. These findings launched continued studies of QC formation and stabilization by experimental shock compression.

The i-QCs in the Al-Fe-Cr ternary are of interest because they form nanoparticles in an aluminum matrix and consequently make composites with the unusual combination of high hardness and good ductility [7]. Unlike the stable $Al_{63}Cu_{25}Fe_{12}$ icosahedrite, i-QCs in the Al-Fe-Cr ternary are metastable. Therefore, considerable of effort has been invested in exploring for quenchable compositions in this ternary system. To date, Al-Fe-Cr i-QC have been successfully synthesized in the high-Al regime with Fe/Cr close to 1, e.g. $Al_5(Cr_{0.5}Fe_{0.5})$ [8], $Al_{98-x}Cr_xFe_2$ (x=3 or 5) [7] and $Al_{93}(Fe_3Cr_2)_7$ [9]. It is also possible to promote the stability of QC via doping with a fourth element, e,g, $Al_{93}Fe_3Cr_2Ti_2$ [9]. However, the effect of copper, particularly as a dopant, in the Al-Fe-Cr system has not received much attention. In this research, we used a functionally graded Al-Cu-W composite (originally a graded density impactor) in a 304 stainless steel shock recovery chamber as starting material, to sample a range of Al/Cu starting ratios and supply Fe, Cr, Ni at the sample-chamber interface. We present detailed *in situ* characterization of the

Shock Compression of Condensed Matter - 2019
AIP Conf. Proc. 2272, 100013-1–100013-4; https://doi.org/10.1063/12.0001005
Published by AIP Publishing. 978-0-7354-4000-5/$30.00

synthesized $Al_{68}Fe_{20}Cr_6Cu_4Ni_2$ i-QC and associated intermetallic phases and discuss the stabilization of i-QC in this composition.

SAMPLE AND METHODS

For the shock recovery experiment, we sliced an Al-Cu-W graded density impactor (GDI) at an oblique angle to form a wedge. The GDI is 3.3 mm in thickness with graded composition from aluminum on top to copper in the middle and to tungsten at the bottom (Fig. 1a). The GDI sample was milled to a disk of 8.2 mm in diameter and then cut diagonally at 22° into two wedge-shaped halves. We used the half with major aluminum/copper and minor tungsten for the shock experiment. An identically-shaped wedge of 304 stainless steel (SS304) was made to back up the GDI wedge (Fig. 1b) and assemble into an overall right circular cylinder to fit in the sample chamber. The Al top of the GDI faced up toward impact surface of the recovery chamber. The wedge-sample is designed to convert the different particle velocities across the GDI/steel interface into a component of interface-parallel sliding and thus create strong shear flow. The sheared zone is expected to enable or enhance melting at the interface and reactions between the metallic phases. The sample assembly was encased in a SS304 chamber and impacted by a tantalum flyer. The impact velocity of 0.93 km/s produced estimated first shock pressures of 14 GPa, 22 GPa and 31 GPa in the aluminum, copper and tungsten portions of the sample, respectively. The pressures were calculated from the measured impedance of the GDI using the WONDY 1-D hydrocode [10–12]. Further experimental details can be found in [12].

The recovery sample was cut through the mirror plane of the GDI wedge. The exposed surface was polished on diamond lapping films and analyzed with a scanning electron microscope (SEM). Energy dispersive X-ray spectroscopy (EDS) was used to measure the chemical composition of the intermetallic phases. We employed electron backscattered diffraction (EBSD) to determine the (quasi)crystal structure of the phases. The shock-recovery experiment and SEM analyses were performed at the Division of Geological and Planetary Sciences in Caltech.

RESULTS

Overall, shock-induced deformation and reaction is concentrated on the corners of the GDI wedge. The long interface between the Al-rich top of the GDI and steel driver is coherent and well-defined without much reaction. In contrast, in areas like the upper-right corner (Fig. 1c), the sample was squeezed along the direction of the impact and strongly deformed. That causes partial melting of the GDI and steel driver and simultaneous reactions between them. Figure 2a extends from a region of unmelted GDI into the area of recrystallized aluminum/copper and intermetallic phases from GDI-driver reactions. The lower-left portion of Fig. 2a shows coarse aluminum grains from the unmelted GDI. The grains generally preserve their original size and are deformed along the direction of impact. Adjacent to the unmelted portion, aluminum occurs as fine grains of several microns with a bright interstitial phase, inferred to be Cu-rich (Fig. 2a). There are also large remnant copper fragments in the matrix of fine-grained aluminum. Closer to the steel capsule wall lies the region of intermetallic phases, which has a curved or lobate boundary against the zone of fine Al grains (Fig. 2a-b). Compositionally, the phases are Al-dominant but incorporate significant iron and chromium plus minor copper and nickel. Therefore, their backscattered electron (BSE) contrast is intermediate between aluminum and copper (Fig 2a).

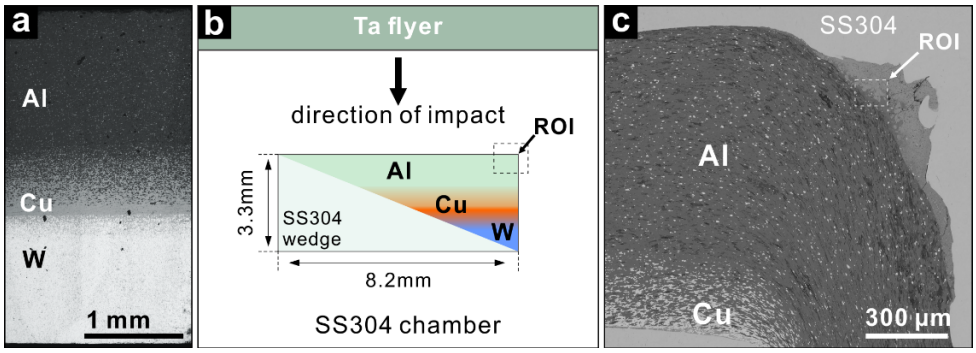

FIGURE 1. (a) SEM image of a cross section of the unshocked Al-Cu-W GDI. (b) Design of the recovery target assembly containing the GDI wedge. The region of interest (ROI) is shown in c. (c) SEM image of the shock-deformed corner of GDI. A reaction zone occurs between the Al-rich portion of the GDI and the steel chamber wall. Details of ROI are in Fig. 2.

Figure 2b shows detailed micro-texture of the Al-Fe-Cr-Cu-Ni intermetallic phases. The phase with high BSE contrast is the icosahedral quasicrystal (i-QC). Its average formula is $Al_{68}Fe_{20}Cr_6Cu_4Ni_2$, with less than 0.2 at% of Si and Mn that cannot be precisely determined. The icosahedral symmetry is indicated by the EBSD pattern with clear 5-fold, 3-fold and 2-fold rotation axes (Fig 2 upper inset). EBSD mapping also indicates that the apparently homogenous and smooth i-QC regions, greater than 10 microns across, are in fact divided into quasicrystalline sub-domains a few microns in size. The polycrystalline phase adjacent to the i-QC (Fig. 2b) is hollisterite (ideally $Al_{13}Fe_4$, $C2/m$), also known as the λ phase in system of notation adopted for Al alloys (Fig. 2 lower inset). Its average formula is $Al_{71}Fe_{18}Cr_5Cu_3Ni_2$, also with minor Si and Mn. Hollisterite forms sub-micron grains, with grain boundaries clearly visible in BSE because they are marked by thin films of high-contrast interstitial (inferred) Fe-Cu alloy.

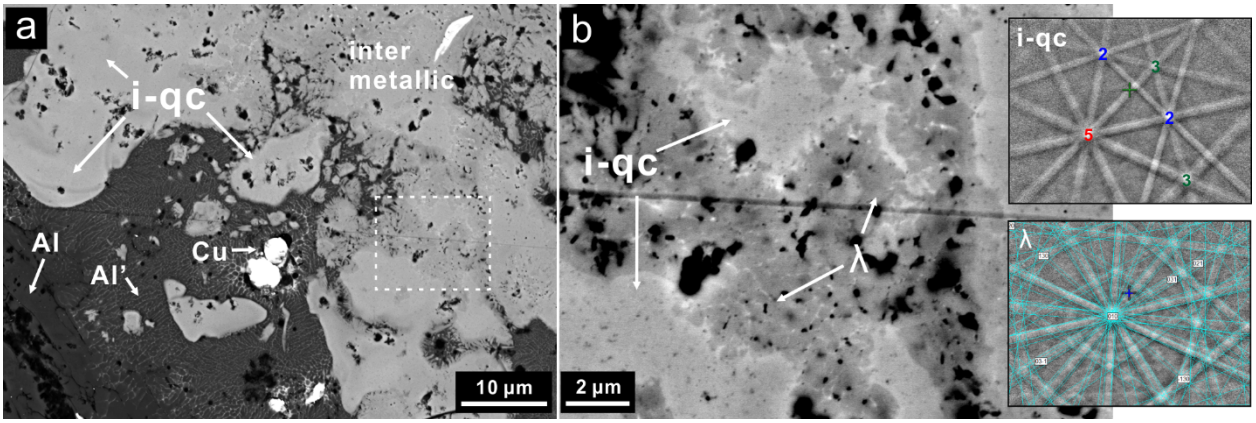

FIGURE 2. (a) BSE image for the melting, recrystallization and reaction (with steel driver) of GDI. The pure Al, pure Cu and Al-Fe-Cr intermetallic phases show low, high and intermediate contrast, respectively. Al and Al' marks remnant and recrystallized aluminum from melt. The boxed area is shown in b. (b) High-magnification BSE image of the icosahedral quasicrystal (i-qc) and hollisterite (λ). The two insets are EBSD patterns for the quasicrystal with 5-fold rotation axis and for hollisterite with plane indices.

DISCUSSION

As in previous occurrences of shock-synthesized i-QC [5,6], the anticipated reactions between the sample and the steel chamber are restricted to areas of strong deformation along the sample boundary. At the shock pressures in question, the homogeneous shock temperature is well below melting; it requires frictional and viscous dissipation in the region of shear to heat the metals and alloys to their melting points [6]. In our sample, a melted zone up to 200 µm wide formed along the Al-rich end of the GDI by shock-induced pore collapse and deformation. In the first 30 µm of the melt zone adjacent to the GDI sample, the originally coarse aluminum and copper grains are only melted and recrystallized to fine Al grains and interstitial Cu without further reaction. That is, the steel melt does not migrate far enough from the chamber wall to mix with all of the Al melt. The Al/Cu at the Al-rich end of the GDI is higher than that of Al-Cu binary intermetallic phases, so they quench to separate metal phases. The rest of the >100 µm wide melt zone is filled with intermetallic phases (Fig. 1c). In this reaction zone, the Al-Fe-Cr-Cu-Ni i-QC is more abundant near the recrystallized Al matrix, whereas the hollisterite (λ) is distributed across the whole reaction zone from GDI to chamber wall. Nevertheless, the i-QC commonly has 2-3 at% higher Fe content than the hollisterite. That may suggest that the melt zone cannot be described as a simple zone of laminar shear flow that preserves a regular linear gradient across its width from Al sample through progressively more steel-rich mixtures to the steel wall. Instead, the different particle velocities in different phases may create complex three-dimensional flow or even turbulence that distributes the steel component across the melt zone.

The texture of the i-QC and hollisterite suggest a possible hypothesis about their formation sequence. Texturally, the quasicrystal domains form continuous smooth regions without well-defined grain boundaries. In contrast, interstices between the hollisterite grains are filled with high-contrast phases (Fig. 2b), inferred to be Cu-rich, e.g. stolperite (β, Al(Cu,Fe)). Besides, the boundary between i-QC and hollisterite is convoluted at a very small scale, making it look "fuzzy" (Fig. 2b). Unlike the synthesis pathway by the distributary peritectic reaction of λ+β+liquid ⇌ icosahedrite ($Al_{63}Cu_{24}Fe_{13}$) [13], the hollisterite and interstitial phases may result from disproportionation of a precursor phase, possibly the Al-Fe-Cr i-QC itself, induced by release of the shock pressure and post-shock annealing.

It is difficult, though, to test the idea that the hollisterite aggregate regions share the bulk composition of the i-QC because the pervasive associated voids (see Fig. 2b) interfere with bulk analysis.

Oppenheim et al. (2017) discussed the stability of Al-Cu-Fe-Cr-Ni quinary QC in the context of Hume-Rothery rules for stability based on valence electron density. The results suggested that nearly equal amounts of Fe and Cu in an i-qc would permit incorporation of more Cr and Ni, up to 25 at%, whereas compositions with high Fe and low Cu would have sharply limited capacity to contain Cr or Ni. In fact, the 20 at% Fe and < 4 at% Cu content in the i-QC from this study place it precisely on the estimated stability boundary of Cr+Ni bearing i-QC, where incorporation of up to 5 at% Cr+Ni should be possible. Given that the effect of pressure on valence electron density and other factors may modify the contraints somewhat, the presence of a total of 8 at% Cr+Ni in our $Al_{68}Fe_{20}Cr_6Cu_4Ni_2$ i-qc seems reasonably consistent with the predictive framework of Hume-Rothery rules. In addition, the Fe:Cr:Ni ratio in the i-QC is close to that of the 304 stainless steel starting material, suggesting limited chemical segregation. The nucleation of a single solid phase by possible congruent crystallization could minimize the need for chemical segregation to form and grow a solid phase and should have a reduced activation energy barrier. Hence, bulk mixing of molten steel with the portion of the GDI where Al is abundantly available and Cu is scarce may have optimally stabilized formation of our low-Cu Al-Fe-Cr quasicrystal. Compared to former shock experiments starting with $CuAl_5$ alloys [5,6], the GDI sample in this experiment is distinguishable by the Al-Cu compositional gradient and, coincidently, a uniform layer of > 90% Al at the front of the wedge (Fig. 1). The latter turned out to be advantageous to explore the i-QC stability at high Al/Cu ratios. Subsequently, as the i-QC underwent post-shock annealing, it may have partly disproportionated to hollisterite, releasing the non-Al elements now found concentrated in the interstices.

Previous studies on synthetic Al-Cr-Fe quasicrystals mostly use Fe/Cr ratio of 1 to 1.5. The logic guiding the focus of work to this part of the composition space has been the usage of the important i-QC approximant α-$Mn_{12}(Al,Si)_{57}$ as a reference for the quasicrystal (meta)stability [2]. Although Mn is not present in Al-Cr-Fe system, it is isoelectronic with an equal mixture of Fe and Cr, and a 1:1 FeCr alloy can crystallize in the α-Mn isomorph structure [8]. Hence, our serendipitous exploration of much higher Fe/Cr ratios, due to the use of SS304 as a precursor, allows our study to show that Al-Fe-Cr quasicrystals can have Fe/Cr ratios much greater than 1.5, at least in the presence of Cu. Further studies with varied impact velocities would better constrain the pressure effects on this i-QC.

ACKNOWLEDGMENTS

We thank NASA Solar System Workings grant 80NSSC18K0532 for supporting this research. The Lindhurst Laboratory for Experimental Geophysics at Caltech is also supported by NSF awards EAR-1725349 and 1829277. We gratefully thank Jeff Nguyen from LLNL for providing the GDI. Constructive comments from the anonymous reviewer are appreciated.

REFERENCES

1. D. Shechtman, I. Blech, D. Gratias, and J.W. Cahn, Phys. Rev. Lett. **53**, 1951 (1984).
2. A.P. Tsai, in *Phys. Prop. Quasicrystals*, edited by Z.M. Stadnik (Springer Berlin Heidelberg, Berlin, Heidelberg, 1999), pp. 5–50.
3. L. Bindi, P.J. Steinhardt, N. Yao, and P.J. Lu, Science **324**, 1306 (2009).
4. L. Bindi, N. Yao, C. Lin, L.S. Hollister, C.L. Andronicos, V.V. Distler, M.P. Eddy, A. Kostin, V. Kryachko, G.J. MacPherson, W.M. Steinhardt, M. Yudovskaya, and P.J. Steinhardt, Am. Mineral. **100**, 2340 (2015).
5. P.D. Asimow, C. Lin, L. Bindi, C. Ma, O. Tschauner, L.S. Hollister, and P.J. Steinhardt, Proc. Natl. Acad. Sci. **113**, 7077 (2016).
6. J. Oppenheim, C. Ma, J. Hu, L. Bindi, P.J. Steinhardt, and P.D. Asimow, Sci. Rep. **7**, 15629 (2017).
7. A. Inoue, H. Kimura, K. Sasamori, and T. Masumoto, Mater. Trans. JIM **37**, 1287 (1996).
8. Chr. Janot, J. Pannetier, J.-M. Dubois, and R. Fruchart, Phys. Lett. A **119**, 309 (1986).
9. M. Galano, F. Audebert, B. Cantor, and I. Stone, Mater. Sci. Eng. A **375–377**, 1206 (2004).
10. M.E. Kipp and R.J. Lawrence, NASA STIRecon Tech. Rep. N **83**, (1982).
11. J.P. Kelly, J.H. Nguyen, J. Lind, M.C. Akin, B.J. Fix, C.K. Saw, E.R. White, W.O. Greene, P.D. Asimow, and J.J. Haslam, J. Appl. Phys. **125**, 145902 (2019).
12. J. Hu, P.D. Asimow, C. Ma, and L. Bindi, IUCrJ (2020 *in press*).
13. L. Zhang and R. Lück, Z. Für Met. **94**, 91 (2003).